

Nonlinear model of acoustical attenuation and speed of sound in a bubbly medium.

Amin Jafari sojahrood, Hossein Haghi, Raffi Karshafian, Michael C. Kolios
 Department of Physics
 Ryerson University
 Toronto, Canada
 amin.jafarisojahrood@ryerson.ca

Abstract— The presence of microbubbles (MBs) in a medium changes the medium's acoustic properties and increases the attenuation of the bubbly medium. Current models of ultrasound attenuation in a bubbly medium are based on linear approximations; that is MB undergoes very small amplitude oscillations. Thus linear models of attenuation are not valid in many regimes used in diagnostic and therapeutic ultrasound applications. In this study, a model is developed that incorporates the nonlinear attenuation and sound speed by deriving the complex wave number from the Calfish model for the propagation of acoustic waves in a bubbly medium. Using the methods of nonlinear dynamics, we have classified the behavior of MBs for a wide range of frequencies and applied pressures. The results of the bubble oscillations are visualized using the bifurcation diagrams of the radial oscillations of the MBs as a function of the incident pressure. It is shown that depending on the frequency of the ultrasound wave, the nonlinear oscillations of the MBs can be classified into 5 main categories in which the MBs oscillations exhibit: 1. Linear resonance (fr), 2. Pressure-dependent resonance (fs), 3. Sub Harmonic (SH) resonance (fSH), 4. Pressure-dependent SH resonance (fpSH) and 5. Higher order SH resonance oscillations (fn). Results show that when MBs are sonicated by their fr, the effective attenuation of the medium can potentially decrease as the pressure increases, which is in good agreement with experimental observations. When sonicated with their fs, the effective attenuation of the medium is smaller than in the case of fr. This happens only below a pressure threshold that corresponds to the saddle node bifurcation in the corresponding bifurcation diagram. Above this pressure, the effective attenuation and sound speed increase abruptly by ~5 and ~2 folds, respectively. In the other classified sonication regimes (fSH, fsSH and fn) (3-5), the attenuation and sound speed changes are negligible below the pressure threshold corresponding to the SH oscillations. As soon as the pressure increases above the threshold for SH oscillations (e.g. period doubling in the bifurcation diagram), the effective attenuation increases abruptly (~ up to 3 fold), however the maximum exhibited attenuation is ~10 to 50 folds smaller than the maximum attenuation in case of sonication with fr and fs.

I. INTRODUCTION

The behavior of microbubbles (MBs) is non-linear and complex [1-6]. Introducing of MBs in a medium changes the acoustic properties of the medium. It increases the attenuation [7-9] of the medium and alters the sound speed [7, 8]. The existing models of ultrasound attenuation in a bubbly medium are based on linear approximations (very small amplitude MB

oscillations-e.g. the Commanser and Prosperetti model [7]). However, in most of the applications (e.g. MB enhanced diagnostic imaging, therapeutic ultrasound and sonochemistry) higher acoustic pressures are employed which result in high amplitude nonlinear MB oscillations. Thus linear models are not valid in many regimes used in applications [8-9].

II. METHODS

A. The nonlinear model for the attenuation and sound speed

Calfish has developed a model [10] for the propagation of an acoustic wave of arbitrary amplitude in a bubbly liquid. The bubbly liquid is described as a continuum, in which the radial oscillations of all the bubbles of an elementary small volume of mixture located at a spatial point r can be explained by a continuous spatio-temporal radius function $R(r,t)$. After elimination of the velocity field between the conservation of mass and momentum equations, the Calfish model [10] can be written as [7]:

$$\nabla^2(P) = \frac{1}{C_l^2} * \frac{\partial^2 P}{\partial t^2} - \rho_l \frac{\partial^2 \beta}{\partial t^2} \quad (1)$$

Where P is the acoustic pressure, c_l is the sound speed of the medium in the absence of the bubbles, ρ_l is the density of the liquid and β is the instantaneous void fraction as is given by eq.

$$\beta = \frac{4}{3} N \pi R(t)^3 \quad (2)$$

Where N is the number of the bubbles per m^3

By deriving the real and imaginary part of the complex wave number from the calfish equation the attenuation and speed of sound can be written as a function of the driving frequency and acoustic pressure and the radial oscillations of the MBs. The time averaged real and imaginary part of k^2 are respectively represented by equations 3 and 4

$$\langle \Re(k^2) \rangle = \frac{-\omega^2}{C_l^2} - \frac{\rho_l}{T * 0.5 * |P|^2} \int_0^T \Re(P) \frac{\partial^2 \beta}{\partial t^2} dt \quad (3)$$

$$\langle \Im(k^2) \rangle = -\frac{\rho_l}{T * 0.5 * |P|^2} \int_0^T \Im(P) \frac{\partial^2 \beta}{\partial t^2} dt \quad (4)$$

Where the operator \Re and \Im are imaginary and real part of the complex number and T is the duration of the pulse.

Using the real and imaginary part of the wave number the pressure dependent nonlinear attenuation and speed of sound in the bubbly medium can simply be derived.

B. Hoff model for the radial oscillations of the microbubbles

The radial oscillations of the MBs as a function of pressure, frequency and the MB initial radius was simulated by numerically solving the Hoff model [11] and considering the additional terms responsible for radiation and thermal damping [12].

$$\rho \left(\left(1 - \frac{\dot{R}}{c}\right) R \ddot{R} + \frac{3}{2} \dot{R}^2 \left(1 - \frac{\dot{R}}{3c}\right) \right) = \left(1 + \frac{\dot{R}}{c} + \frac{R}{c} \frac{d}{dt}\right) (P_g - p_A(t)) - 4\mu_L \frac{\dot{R}}{R} - 12\mu_s \theta \frac{R_0^2}{R^3} \frac{\dot{R}}{R} - 12G_s \theta \frac{R_0^2}{R^3} \left(1 - \frac{\dot{R}}{R}\right) \quad (5)$$

Where:

$$\begin{aligned} \dot{P}_g &= \gamma P_g \left(\frac{-3\dot{R}}{R} \right) + \frac{3\lambda(\gamma-1)(T-T_0)}{R} \sqrt{\frac{3(\gamma-1)|\dot{R}|}{R\alpha}} \\ \dot{T} &= \frac{4\pi R^2}{C_V} \left[\lambda \frac{T_0 - T}{l_{th}} - \dot{R} P_g \right] \\ l_{th} &= \min \left(\sqrt{\frac{R\alpha}{|\dot{R}|}}, \frac{R}{\pi} \right) \end{aligned} \quad (5)$$

The parameters of this equation are summarized in table 1.

The results of the numerical simulations were visualized using the bifurcation diagrams.

| | | |
|-----------|-------------------------------|----------------------------------|
| R_0 | Initial radius | 2.5(μm) |
| ρ | Liquid density | 998(kg/m^3) |
| c | Sound speed | 1500(m/s) |
| P_{g0} | Gas pressure | 1.01e5 (Pa) |
| μ_L | Liquid viscosity | 0.001(Pa.s) |
| μ_s | Shell viscosity | 0.95(Pa.s) |
| θ | Shell thickness | 4(nm) |
| G_s | Shell shear modulus | 45(MPa) |
| γ | Polytropic Exponent | 1.095 |
| λ | Gas conductivity | 0.016(W/mK) |
| T_0 | Initial temperature | 300(K) |
| α | Thermal gas diffusivity | 3.83e-5(m^2/s) |
| C_V | Specific heat at constant V | 0.312(KJ/kg K) |
| l_{th} | Thermal diffusion length at t | (m) |

Table 1: Parameters of equation 2 and 3.

III. RESULTS

Figure 1 shows the bifurcation diagram of the normalized radial oscillations of the MB as a function of acoustic pressure at different frequencies. Depending on the frequency of the ultrasound wave, the nonlinear oscillations of the MBs can be classified into 5 main categories where the MBs exhibit (fig 1):

1. Linear resonance ($f_r=2.4$ MHz – blue line).
2. Pressure dependent resonance ($f_s=1.9$ MHz- red line) [13]

3. Sub Harmonic (SH) resonance ($f_{SH}=4.8$ MHz- black line)
4. Pressure dependent SH resonance ($f_{pSH}=3.6$ MHz-green line) and
5. Higher order SH resonance oscillations ($f_3= 6.3$ MHz- brown line and $f_4 = 8$ MHz-light orange line).

When sonicated with f_r , as the pressure increases, the radial oscillations of the MB increases and the oscillations undergo a period doubling bifurcation at ~ 300 kPa. The MB undergoes a possible collapse at ~ 430 kPa as the normalized radial oscillations of the MB pass the destruction threshold ($R/R_0 > 2$) [14]. The corresponding attenuation behavior of the medium is shown in a blue line in Figure 2. When the MB is driven at its f_r , the attenuation is maximum at the lower sonication pressures. As the pressure increases, the attenuation decreases. The attenuation decreases further which is concomitant with period doubling.

The sound speed when sonicated at f_r (blue line in Figure 3) is equal to the sound speed of the liquid at very low pressures < 1 kPa. As the pressure increases the normalized sound speed c/c_l (speed of sound in the bubbly liquid/sound speed of the pure liquid) increases to ~ 1.5 . As the pressure increases further the sound speed undergoes a decrease concomitant with the period doubling.

When the MB is sonicated with its pressure dependent resonance frequency [13] (1.9 MHz- red line in figure 1) the radial oscillation amplitude undergoes a sudden increase via a saddle node bifurcation at ~ 115 kPa. The MB oscillations pass the destruction threshold at ~ 270 kPa. The corresponding attenuation (red line in figure 2) is small compared to the case of linear resonance only below the pressure threshold for the saddle node bifurcation. The attenuation increases abruptly (~ 5 times) concomitant with the saddle node bifurcation at ~ 115 kPa. The attenuation starts decreasing slowly as the pressure increases $> \sim 120$ kPa.

The normalized sound speed (c/c_l) is ~ 0.8 only when the pressure is below the pressure threshold for saddle node bifurcation. Above this pressure the sound speed grows abruptly and reaches ~ 2.1 . At the saddle node bifurcation pressure the sound speed of the bubbly liquid is equal to the speed of sound in the pure liquid.

When the MB is sonicated by its SH resonance frequency ($f_{SH}=4.8$ MHz the black line in fig. 1) The period doubling occurs at the lowest pressure threshold ~ 160 kPa compared to other frequencies. The radial oscillations undergo further period doublings to chaos at ~ 730 kPa. The attenuation of the medium (black line in figure 2) is significantly lower than the case of f_r and f_s . As soon as period doubling occurs, the attenuation increases abruptly by ~ 2 fold. Further increase in pressure results in a slight decrease in attenuation.

When sonicated with 3.6 MHz (green line in figure 1) the radial oscillations of the MB undergo a saddle node bifurcation to period 2 oscillations at ~ 330 kPa. The corresponding attenuation in figure 2 (green line) abruptly increases (~ 3 fold) concomitant with saddle node bifurcation.

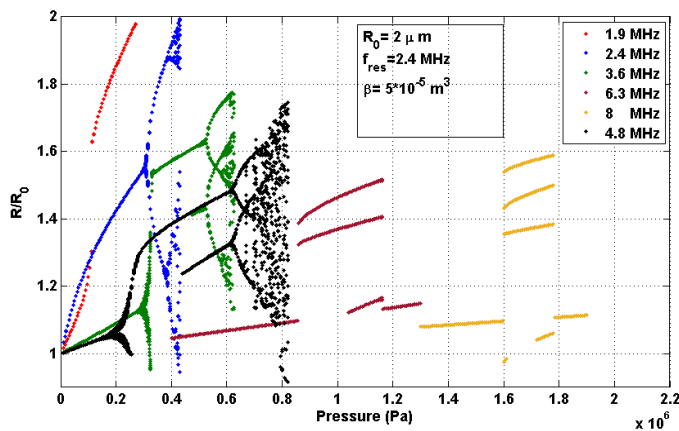


Figure 1: Bifurcation diagram of the radial oscillations of the MB versus the driving acoustic pressure. Every color represents a different frequency.

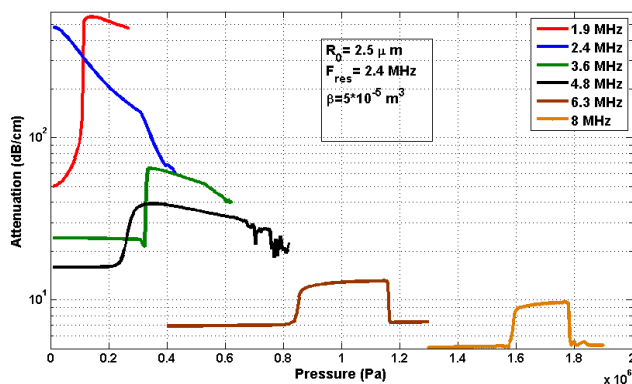


Figure 2: Attenuation of the bubbly medium versus pressure at different frequencies. Pressure ranges for attenuation calculation are extracted from the bifurcation diagrams.

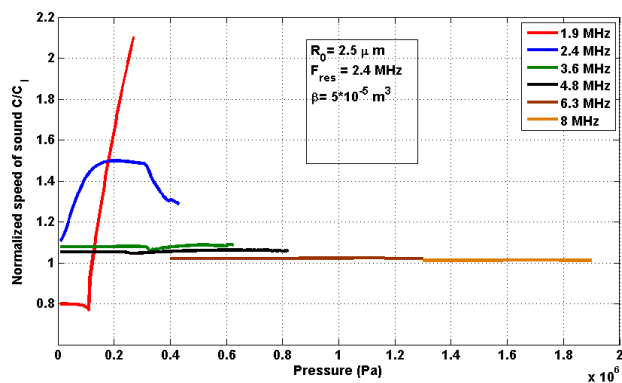


Figure 3: Normalized speed of sound (c/c_0) of the bubbly medium versus pressure at different frequencies. Each color represents a different frequency.

When the MBs are sonicated with frequencies slightly less than 3 and 4 times its linear resonance, higher order SH responses of respectively 1/3 and 1/4 occur in the radial oscillations [15]. For sonication frequency of 6.3 MHz (brown line in fig 1) the MB exhibits period 3 oscillations (1/3 SHs) for pressure levels above ~ 855 kPa. The attenuation of

the medium undergoes an increase (~ 2 times) concomitant with period 3 oscillations.

When MBs are sonicated with 8 MHz (light orange line in fig. 1), the radial oscillations of the MB exhibits period 4 oscillations for acoustic pressures above 1.6 MPa. The attenuation of the medium undergoes a sharp increase (~ 1.7 fold) as soon as MB exhibits period 4 oscillations.

The changes in the speed of sound is more emphasized in case of sonication with f_s and f_r and it is negligible for higher frequencies (fig. 3)

IV. DISCUSSION AND SUMMARY

The acoustic response of MBs strongly depends on the ultrasound frequency and pressure. It is shown that the nonlinear oscillations of the MBs can be classified into 5 main categories depending on the sonicated frequency in which MBs exhibit: 1. Linear resonance (f_r), 2. Pressure-dependent resonance (f_s), 3. Sub Harmonic (SH) resonance (f_{SH}), 4. Pressure-dependent SH resonance and 5. Higher order SH resonance oscillations (f_n). The results show that when MBs are sonicated at their f_r , the effective attenuation of the medium can potentially decrease as the pressure increases, which is in good agreement with experimental observations [16]. When sonicated with their f_s , the effective attenuation of the medium is smaller than in the case of f_r . This happens only below a pressure-threshold that corresponds to the saddle node bifurcation in the associated bifurcation diagram. Above this pressure, the effective attenuation and sound speed increase abruptly by ~ 5 and ~ 2 folds, respectively. In the other classified sonication regimes (3-5), the attenuation and sound speed changes are negligible below the threshold corresponding to the SH oscillations. As soon as the pressure increases above the threshold for SH oscillations (e.g. period doubling in the bifurcation diagram), the effective attenuation increases abruptly (\sim up to 3 fold), however the maximum exhibited attenuation is ~ 10 to 50 folds smaller than the maximum attenuation in case of sonication with f_r and f_s .

The changes of the attenuation and speed of sound of a bubbly medium are nonlinear and depend on frequency and pressure. Linear models (e.g Commander and Prosperetti [7]) are only valid for small amplitude oscillations and they cannot capture the significant changes in attenuation as the pressure increases. The semi-linear model developed by Louisnard [8] can capture the pressure dependent imaginary part of the wavenumber; however it still uses the linear model to estimate for the real part of the wave number. It was shown that the speed of sound exhibits strong pressure dependence when the bubbly medium is sonicated with f_s and f_r . Thus the semi-linear model will fail in capturing the attenuation accurately at these regimes.

REFERENCES

[1] Parlitz, U., Englisch, V., Scheczyk, C., Lauterborn, W.: Bifurcation structure of bubble oscillators. J. Acoust. Soc. Am. 88(2), 106177 (1990)

- [2] Lauterborn, W., Suchla, E.: Bifurcation structure in a model of acoustic turbulence. *Phys. Rev. Lett.* 53(24), 2304–2307 (1984). J. Clerk Maxwell, *A Treatise on Electricity and Magnetism*, 3rd ed., vol. 2. Oxford: Clarendon, 1892, pp.68–73.
- [3] Holt, R.G., Gaitan, D.F., Atchley, A.A., Holzfuss, J.: Chaotic sonoluminescence. *Phys. Rev. Lett.* 72(9), 13769 (1994).
- [4] Behnia, S., Jafari, A., Soltanpoor, W., Jahanbakhsh, O.: Nonlinear transitions of a spherical cavitation bubble. *Chaos, Solitons Fractal* 41, 818–828 (2009)
- [5] Behnia, S., Jafari, A., Soltanpoor, W., Sarkhosh, L.: Towards classification of the bifurcation structure of a spherical cavitation bubble. *Ultrasonics* 49, 605–610 (2009)
- [6] Hegedűs, F., Hóros, C., Kullmann, L.: Stable period 1, 2 and 3 structures of the harmonically excited Rayleigh–Plesset equation applying low ambient pressure. *IMA J. Appl. Math.* 78(6), 1179–1195 (2013)
- [7] K.W. Commander, A. Prosperetti, Linear pressure waves in bubbly liquids: comparison between theory and experiment, *J. Acoust. Soc. Am.* 85 (2) (1989) 732–746.
- [8] O. Louisnard, A simple model of ultrasound propagation in a cavitating liquid. Part I: Theory, nonlinear attenuation and traveling wave generation *Ultrason. Sonochem.*, 19 (2012), pp. 56–65
- [9] R. Jamshidi, G. Brenner, Dissipation of ultrasonic wave propagation in bubbly liquids considering the effect of compressibility to the first order of acoustical Mach number *Ultrasonics*, 53 (2013), pp. 842–848
- [10] R.E. Caflish, M.J. Miksis, G.C. Papanicolaou, L. Ting Effective equations for wave propagation in bubbly liquids *J. Fluid Mech.*, 153 (1985), pp. 259–273
- [11] Hoff, L., Sontum, P.C., Hovem, J.M.: Oscillations of polymeric microbubbles: effect of the encapsulating shell. *J. Acoust. Soc. Am.* 107(4), 2272–2280 (2000)
- [12] T.J. Matula, P.R. Hilmo, B.D. Storey, A.J. Szeri
Radial response of individual bubbles subjected to shock wave lithotripsy pulses in vitro *Phys. Fluids*, 14 (2002), pp. 913–92
- [13] A.J. Sojahrood, O. Falou, R. Earl, R. Karshafian, M.C. Kolios
Influence of the pressure-dependent resonance frequency on the bifurcation structure and backscattered pressure of ultrasound contrast agents: a numerical investigation
Nonlinear Dyn., 80 (1–2) (2015), pp. 889–904
- [14] Flynn, H.G., Church, C.C.: Transient pulsations of small gas bubbles in water. *J. Acoust. Soc. Am.* 84, 985–998 (1988)
- [15] A.J. Sojahrood, M.C. Kolios Classification of the nonlinear dynamics and bifurcation structure of ultrasound contrast agents excited at higher multiples of their resonance frequency *Phys. Lett. A*, 376 (33) (2012), pp. 2222–2229
- [16] Y Gong, M Cabodi, TM Porter, Acoustic investigation of pressure-dependent resonance and shell elasticity of lipid-coated monodisperse microbubbles, *Applied Physics Letters* 104 (7), 074103